Observation of multiplex photon by ICCD

Kazufumi Sakai

Corresponding author E-mail: ksakai1958@gmail.com

Abstract

The image intensifier is a revolutionary device that allows direct observation of the particle nature of photons. This outstanding instrument can simultaneously detect the presence and position of photons, which has greatly improved the study of interference at the photon level. However, this instrument can not measure the energy or wavelength of the photon, so even if multiple photons are detected at the same location, it is still detected as one. We found that the histogram of the ratio of the total light intensity to the peak value of the individual fluorescence images obtained by the image intensifier splits into two peaks. We show that this peak splitting occurs with a high probability near the bright line of the interference fringes and can be explained by the continuous photon incidence.

***Keywords*:** photon, interference light, image intensifier, fluorescence intensity

1. Introduction

The particle and wave nature of light has been the subject of much controversy [1,2,3], but the development of the image intensifier (I.I.) [4] verified the interference effects of single photons [5,6,7] and led to dramatic advances in physics and quantum mechanics. Subsequently, the Intensified CCD (ICCD), which combines an image intensifier and a charge-coupled device (CCD), was developed, facilitating the observation of photons. In recent years, the development of Timepix [8,9], a device that detects photons at high speed, has been underway. In ICCDs, individual photons are detected as fluorescent images. Fluorescence gradually decreases with time due to the diffusion effect of excited electrons and the progress of recombination. Therefore, it is not possible to estimate the number of photons from the light intensity (when multiple photons arrive at the same location) because the fluorescence

intensity varies with the ICCD detection timing and exposure time even for the same photon. We found that when photons were imaged with exposure times shorter than the afterglow time of the ICCD, the histogram of the ratio of the peak value to the total light intensity of the individual photon images split into two peaks. We measured the dependence of this effect on the exposure time and the probability of this effect occurring for different types of light (normal light (unmodified), double-slit interference light, and multiple reflection interference light). In the Discussion section, we show that this effect occurs when photons arrive at the same location consecutively.

2. Measurement of light intensity by image intensifier

Figure 1 shows a schematic of the structure of the I.I. The I.I. is designed to obtain an undistorted image by placing a photocathode, which converts light into electrons, a microchannel-plate (MCP), which multiplies electrons, and a phosphor-screen, which converts electrons into light, close together in a ceramic vacuum container. The electrons multiplied by the MCP strike the phosphor-screen, and light corresponding to the number of electrons is output. The output image is enhanced tens of thousands of times compared to the incident optical image.

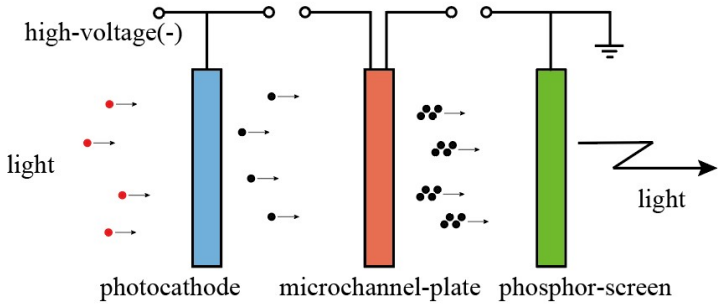

Fig. 1. Structure of an image intensifier. Photons from a low-intensity light source strike a photocathode and emit electrons. Electrons accelerated by high voltage strike the microchannel plate and multiple electrons are emitted. The electrons are attracted to the phosphor-screen by the potential difference and emit fluorescence at the phosphor surface.

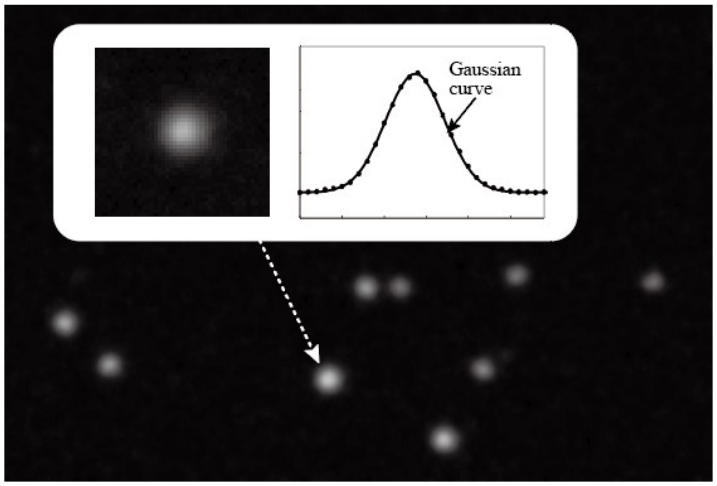

Fig. 2. The image is an example of a group of photons imaged by ICCD. Individual photons can be determined, but their intensities vary. The graphs show the intensity distribution of a single photon (black dots) and the Gaussian approximation curve (solid line).

Figure 2 shows an example of weak light observed by ICCD. As shown in the approximation curve, the fluorescence intensity can be approximated almost by a Gaussian curve. Although multiple photons are detected, the intensity varies. This is due to the temporal decay of fluorescence. If the fluorescence lifetime is τ and the fluorescence intensity at t=0 is A, the temporal variation of the fluorescence intensity L(t) is given by

$$L(t) = A\exp\left(-\frac{t}{\tau}\right) \tag{1}$$

In addition, the excited electrons on the phosphor-screen diffuse into the surrounding area, and the fluorescent image expands with time. This effect is given by the following equation, where the density of excited electrons is ϕ, the diffusion coefficient is D, and the origin of the coordinate (x,y) is the center of fluorescence.

$$\phi(x,y,t) = \frac{1}{4\pi D(t+t_0)}\exp\left(-\frac{(x^2+y^2)}{4D(t+t_0)}\right) \tag{2}$$

where t_0 (>0) is a constant that gives the initial electron distribution at the phosphor-screen (if t_0=0, then equation (2) becomes a δ function at t=0). Thus, the temporal and spatial variation of the fluorescence intensity I(x,y,t) is given by

$$I(x,y,t) = GI_0 \frac{1}{4\pi D(t+t_0)} \exp\left(-\frac{(x^2+y^2)}{4D(t+t_0)}\right) \exp\left(-\frac{t}{\tau}\right) \tag{3}$$

where $I_0/4\pi Dt_0$ is the fluorescence intensity at (x,y,t)=(0,0,0) and G is a parameter that depends on the ICCD. Assuming that t=0 is the time when the electrons arrive at the phosphor-screen, the total fluorescence I_S and the peak intensity I_P at time $t=t_1$ are given by

$$I_S(t_1) = G\int_{-\infty}^{\infty}\int_{-\infty}^{\infty} I(x,y,t_1)dxdy = GI_0 \exp\left(-\frac{t_1}{\tau}\right) \tag{4}$$

$$I_P(t_1) = GI_0 \frac{1}{4\pi D(t_1+t_0)} \exp\left(-\frac{t_1}{\tau}\right) \tag{5}$$

Both I_S and I_P decrease with time. Thus, it can be seen that the light intensity changes at different measurement times.

The ratio I_{PS} in equations (4) and (5) is defined as

$$I_{PS}(t_1) = \frac{1}{4\pi D(t_1+t_0)} \tag{6}$$

If the afterglow time is η (the time until the light intensity reaches 10%), t_1 is random and occurs evenly in the range 0~η, so the probability distribution (histogram with I_{PS} on the horizontal axis and probability of occurrence on the vertical axis) of I_{PS} must be uniform and continuous in the range $1/4\pi Dt_0 \sim 1/4\pi D(\eta+t_0)$ and zero otherwise. However, as shown in the experiment in the next chapter, two peaks appear in the I_{PS} probability distribution when the exposure time is short.

3. Experiments

Figure 3 shows an overview of the apparatus. The light emitted from the semiconductor laser (635 nm, 1 mW) is intensity-adjusted by two Glan-Thompson polarizers (the average number of photons per image is 4.3), and the laser width is adjusted by a line generator (30° in a horizontal direction) and a slit. The light beam is multiply reflected by a half-mirror and a mirror, passes through a fiber optic plate (FOP), and is measured by an ICCD (HAMAMATSU C2400, with a quantum efficiency of about 10% and an afterglow time η of the phosphor-screen is about 1 ms). Figure 4 shows an example of the obtained multiple reflection interference fringes. The spacing of the interference fringes is determined by the relative angles of the mirror and the half-mirror. After removing background noise from the obtained

image, the photon positions are recognized as rectangles, and the sum of the intensities within the rectangles, I_S, and the peak intensity, I_P, are recorded. Images were measured 1000 times, and the I_S and I_P of each photon obtained in each image were statistically processed. The histogram of I_P/I_S versus exposure time T_E of the ICCD is shown in Figure 5(a). When the exposure time is 20 ms, there is only one peak, but as the exposure time decreases, the left peak gradually moves to the right and a second peak appears.

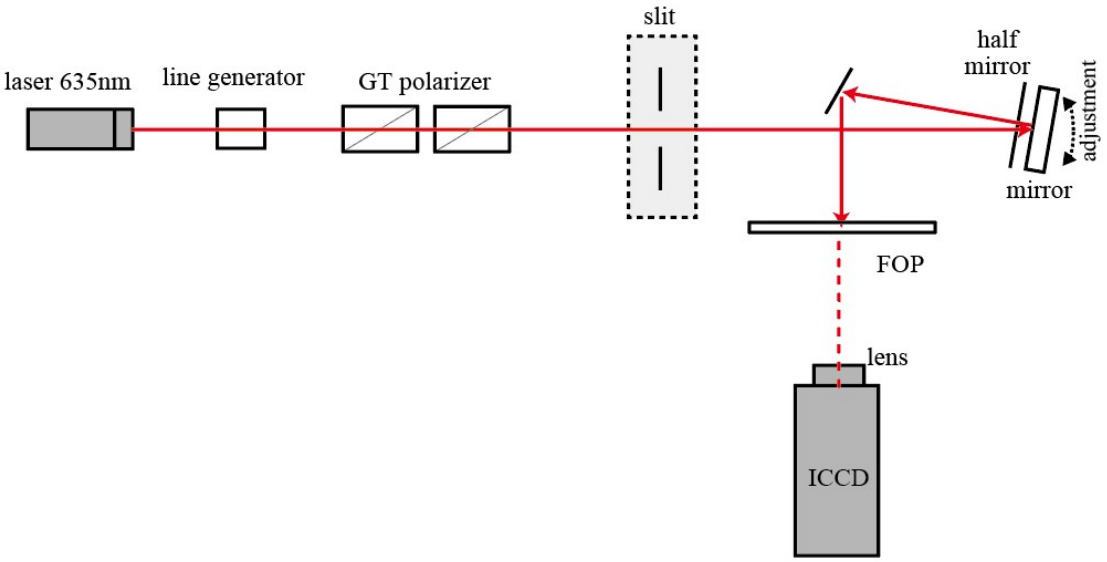

Fig. 3. Light emitted from the laser (635 nm, 1 mW) is spread horizontally by a line generator, and its intensity is adjusted by Glan-Thompson polarizers. The light, whose width is adjusted by the slit, is repeatedly reflected by the half-mirror and mirror and enters the FOP.

Fig. 4. The image was obtained by superimposing the photon positions after imaging the multiple reflection interference light 100 times with the ICCD (each photon was drawn with the same luminance). Interference fringes due to photons can be observed.

Figure 5(b) shows the results of the measurement of the incident beam (unmodified) after

removing the half-mirror from the experimental apparatus shown in Figure 3, as well as the results when a double slit (100um spacing) is placed in front of the FOP. The direct beam and double-slit interference also show a weak peak near I_{PS}=0.23, but it is much smaller (about 20%) than that of the multiple reflection interference light.

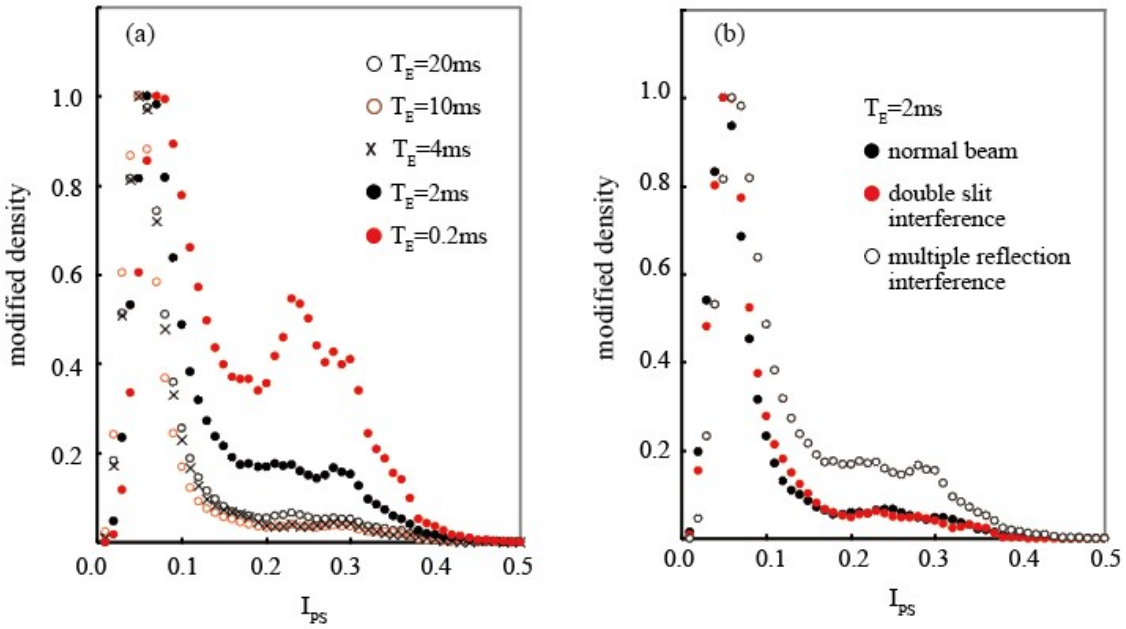

Fig. 5. (a) Probability of I_{PS} occurrence when the exposure time T_E of ICCD is varied in multiple reflection interference light. The second peak appears around I_{PS}=0.23 and gradually increases when the exposure time is equal to or less than the afterglow time of fluorescence. (b) Probability of I_{PS} occurrence for normal beam (no interference), double-slit interference light, and multiple reflection interference light when the exposure time is fixed at 2 ms. The peaks near I_{PS}=0.23 for normal beam and double-slit interference light are very weak. The highest value of each measurement is set as 1 in the graph.

4. Discussion

As shown in the histogram in Figure 5(a), when the exposure time is sufficiently longer than the fluorescence afterglow time, a peak appears near 0.07. When the exposure time becomes shorter (~afterglow time), a peak around 0.23 appears and gradually increases. This second peak is also observed in normal beam and double slit interference light, but it is very small. To illustrate this phenomenon, consider the case of two photons successively incident at the same location.

Figure 6 shows the light intensity decay curves for a single photon incident and two photons incident with a time difference of δt. In the case of a single photon incident, the ratio

of the total light intensity detected at the ICCD to the peak value is given by the following equation using equations (4) and (5).

$$\frac{\int_{t_1-T_E/2}^{t_1+T_E/2} GI_0 \frac{1}{4\pi D(t_1+t_0)} \exp\left(-\frac{t_1}{\tau}\right) dt_1}{\int_{t_1-T_E/2}^{t_1+T_E/2} GI_0 \exp\left(-\frac{t_1}{\tau}\right) dt_1} \tag{7}$$

Similarly, when two photons are incident, I_{PS} is given by

$$\frac{\int_{t_1-T_E/2}^{t_1+T_E/2} \left[GI_0 \frac{1}{4\pi D(t_1+t_0)} \exp\left(-\frac{t_1}{\tau}\right) + GI_0 \frac{1}{4\pi D(t_1+t_0-\delta t)} \exp\left(-\frac{t_1-\delta t}{\tau}\right) \right] dt_1}{\int_{t_1-T_E/2}^{t_1+T_E/2} \left[GI_0 \exp\left(-\frac{t_1}{\tau}\right) + GI_0 \exp\left(-\frac{t_1-\delta t}{\tau}\right) \right] dt_1} \tag{8}$$

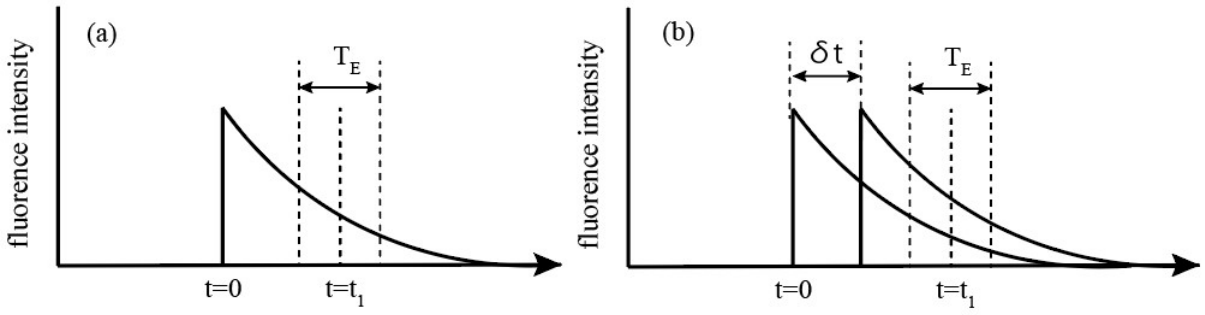

Fig. 6. (a) Schematic of the temporal decay of fluorescence when a single photon enters the phosphor-screen at t=0. The temporal location of the exposure and the decay of fluorescence when the image is taken with exposure time T_E centered at $t=t_1$. (b) Temporal location of exposure and fluorescence decay when two photons enter the same location with a δt delay.

In equation (8), if T_E is sufficiently large compared to τ, the first and second terms in the numerator and denominator are almost identical. Therefore, equation (7) is almost identical to equation (8), and the histogram of I_{PS} has a single peak. On the other hand, if the exposure time is short, the following equation can be obtained by omitting the integral in equation (8).

$$\frac{I_0 \frac{1}{4\pi D(t_1+t_0)} \exp\left(-\frac{t_1}{\tau}\right) + I_0 \frac{1}{4\pi D(t_1+t_0-\delta t)} \exp\left(-\frac{t_1-\delta t}{\tau}\right)}{I_0 \exp\left(-\frac{t_1}{\tau}\right) + I_0 \exp\left(-\frac{t_1-\delta t}{\tau}\right)}$$

$$= \frac{1}{4\pi D(t_1+t_0)} \left\{ 1 + \frac{\frac{t_1+t_0}{t_1+t_0-\delta t} \exp\left(\frac{\delta t}{\tau}\right)}{1+\exp\left(\frac{\delta t}{\tau}\right)} \right\} \tag{9}$$

The second term in parentheses in equation (9) is greater than zero, so equation (9) is always greater than equation (6). Therefore, the IPS histogram moves to the right side, resulting in two peaks. As an example, for $t_1 = t_0 = \tau = \delta t$, the value in parentheses in equation (9) is about 2.5.

Figure 7 shows a graph of where this I_{PS} value is higher in the interference fringes. The I_{PS} values in the graph are averages for each position. It shows that there is a high correlation between interference intensity and I_{PS}. In other words, the peak near I_{PS}=0.23 in Figure 5 occurs near the bright line of the interference fringes.

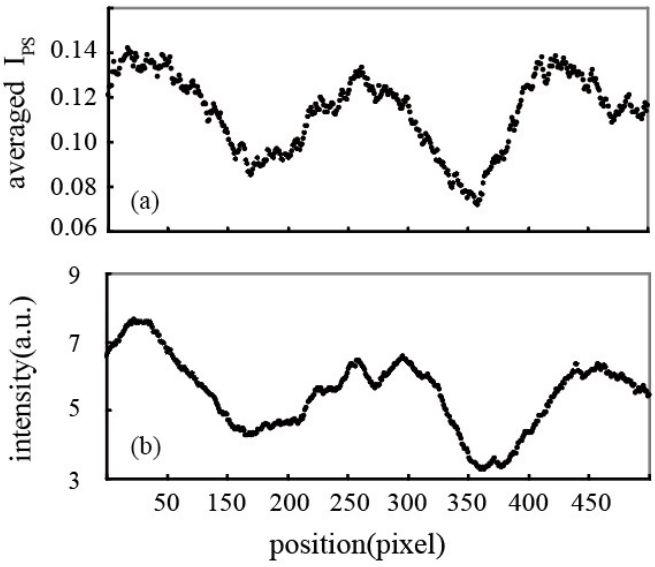

Fig. 7. (a):averaged I_{PS} of individual photons obtained at each position, (b): integrated number of photons at each position. It can be seen that I_{PS} is higher near the bright line of the interference fringes.

Thus, the two peaks can be explained by consecutive incoming photons. However, the

average number of photons measured in one exposure was about 4.3. The probability of two photons entering the same position on the screen is about 0.2%, even taking into account a quantum efficiency of 10%, which cannot explain the experimental results. If the cause of the two peaks is attributed to the ICCD apparatus, the same experimental results must be obtained with normal beam and double-slit interferometry, so the characteristics of the apparatus are not the cause of the occurrence of the two peaks. Therefore, the reason for the second peak is not the accidental incidence of two consecutive photons, but the special state of one photon is considered to be involved.

When measuring photon counts using ICCD, we have shown that multiple photons may correspond to a single photon image and that this effect occurs with high probability in multiple reflection interferometry. Further investigation is necessary to determine the cause of this phenomenon.

REFERENCES

[1] J. Bell, "Against 'measurement'", Physics World, **3** (8), 33–41 (1990)

[2] T. Maudlin, "Why Bohm's Theory Solves the Measurement Problem", Philosophy of Science. **62** (3), 479–483 (1995).

[3] K. Sakai, "Simultaneous measurement of wave and particle properties using modified Young's double-slit experiment", Journal for Foundations and Applications of Physics **5**, 49-54 (2018).

[4] I. P. Csorba, "*Selected Papers on Image Tubes*" (S.p.i.e. Milestone Series), SPIE-The International Society for Optical Engineering (July 31, 1990).

[5] S. Parker, "A Single-Photon Double-Slit Interference Experiment", American Journal of Physics **39**, 420–424 (1971).

[6] P. Grangier, G. Roger and A. Aspect, "Experimental evidence for a photon anticorrelation effect on a beam splitter: a new light on single-photon interferences", Europhys. Lett. **1**, 173–179 (1986).

[7] C. K. Hong, Z. Y. Ou and L. Mandel , "Measurement of subpicosecond time intervals between two photons by interference", Phys. Rev. Lett. **59**, 2044–2046 (1987).

[8]LlopartX. et al., "Timepix, a 65k programmable pixel readout chip for arrival time, energy and/or photon counting measurements", Nucl. Instrum. Methods Phys. Res. A, (2007)

[9]JungmannJ.H. et al., "Fast, high resolution mass spectrometry imaging using a medipix pixelated detector", J. Am. Soc. Mass Spectrom.(2010).